Supplemental Material for Deka et al.

TABLE S1
Oligonucleotide primers used for RT PCR in this study

Primer name	5’ to 3’ sequence
TP0954F	CAAAGAGCGCACCTAAGAGC
TP0956R	AGGGACTGGGCGACTAAATC
TP0956F	GAACACCTTACGCGGTACTG
TP0957R	ATCAAGAGGAGCTGCCTGAC
TP0957F	CAGACTATCGCCCTTTCCAG
TP0958R	GAGAACACCTCGGAACCTAC
TP0958F	CGCCGATTGGAATGAACTTG
TP0959R	CGCTGTTTGTGAGAGTGATG

TABLE S2
N-terminal sequences of Tp0956 and Tp0957

Protein	N-terminal sequence (last residue is putatively lipidated)[a]
Tp0956	MKHPSVRVCCFAFASCLLCAGC
Tp0957	MRTYFFMSVCSVLTC

[a]See Setubal *et al.*[1]

Table S3. Identities of residues whose side chains line the HA of Tp0956 or a cavity in Tp0957

Tp0956 HA	Tp0957 Cavity A	Tp0957 Cavity B	Tp0957 Cavity C
F32	S16	I17	W138
T33	I17	P19	L163
F36	W24	W24	D167
T37	L28	S80	V202
V45	V78	C81	H203
L49	I131	Y94	L204
V52	T132	L96	
L53	T134	S97	
Y56	A136	A136	
L76	L163	L139	
M79	I228	L160	
A83	M230	S162	
F84	L231	L163	
L280	A252	D164	
L281	V255	L168	
L284	L259	L200	
		V202	
		C224	
		P225	
		A226	
		V227	
		I228	

Supplemental Figure Legends

Supplemental Figure S1. Dimensions of the Tp0956 pore. A graph of the pore diameter with respect to the distance from the N-side opening. The pore diameters and path were calculated using the program HOLE [2].

Supplemental Figure S2. Sequence alignment of the cTPR motifs of Tp0956. At the top is the sequence signature of canonical TPR motifs. The red letters are from Sikorski [3], while the blue ones are the consensus sequence derived elsewhere [4]. The bottom four lines show the Tp0956 sequences that have structural homology to TPR motifs. Residue

numbers are given on the right and left sides of the sequences. A boxed letter in red represents a match to the red consensus, and letters shaded in cyan represent matches to the blue consensus. On the right side is also listed the length of the cTPR motif (L), and the rms deviation (RMSD) from the respective motifs in the structures whose accession numbers are shown.

Supplemental Figure S3. The hydrodynamic behavior of Tp0956 alone in the presence of detergent. About 95% of the material sediments with an $s_{20,w}$ of 5.8 S, indicating a trimer of Tp0956.

Supplemental Figure S4. The lack of co-migration of Tp0956 and Tp0655. The $c(s)$ distributions shown here are normalized such that the maximum value for the Tp0956 peak is 1. The black distribution is Tp0956 alone. The magenta distribution is a mixture of Tp0655, which is known to have an $s_{20,w}$-value of 3.2 S, and Tp0956. No movement is shown for the Tp0956 peak, indicating that, in the presence of an excess of Tp0655, there was no detectable interaction between the proteins.

Supplemental Figure S5. TDE1020 and TDE1021 interact. These $c(s)$ distributions have been normalized such that the maximum value of the TDE1021 (the *T. denticola* homolog of Tp0956) peak is 1. The black distribution shows the SV experiment performed on TDE1021 alone. There is a mixture of species; they likely represent trimer (5.8 S) and hexamer (8.2 S). The red distribution represents the experiment performed in the presence of a molar excess of TDE1020 (the *T. denticola* homolog of Tp0957); free TDE1020 is found at 2.8 S (it is monomeric). The TDE1021 peaks are shifted toward faster-sedimenting species, indicating an interaction between TDE1021 and TDE1020.

Supplemental Figure S6. The Lamm-equation fit to the SV data for wild-type Tpo0956 and Tp0957 mixtures. The concentration of Tp0956 was held constant at 0.7 mM, while that of Tp0957 was 0.7, 1.4, 2.1, 3.5, 7, 10.5, and 14 μM. Only the 0.7 (A), 3.5 (B), and 14 μM (C) experiments are shown. The x-axes of the graphs are the distances from the center of rotation in cm, and the y-axes in the upper parts are absorbance values. The y-axes in the lower parts are the residual between the data and the fits, also in absorbance units. The filled-in circles are individual data points, and the lines are the fits to these data; both are color-coded with reverse-rainbow colors, such that early scans are shown in violet, and late scans in red. The fits are global, i.e. a single set of parameters (see Materials & Methods) was used to fit to all seven data sets. For the sake of clarity, only every third data point and every third scan used in the analysis are shown.

Supplemental Figure S7. The phylogenetic tree of P proteins. The proteins are named by their TRAP database number or by their PDB accession code, where appropriate. The P-proteins associated with Tp0956 homologs are named by their locus tag. This clade is colored in red. A scale representing the number of substitutions per site is given in the lower-right corner.

Supplemental References

1. Setubal, J. C., Reis, M., Matsunaga, J. & Haake, D. A. (2006). Lipoprotein computational prediction in spirochaetal genomes. *Microbiology* **152**, 113-121.
2. Smart, O. S., Goodfellow, J. M. & Wallace, B. A. (1993). The pore dimensions of gramicidin A. *Biophysical Journal* **65**, 2455-2460.
3. Sikorski, R. S., Boguski, M. S., Goebl, M. & Hieter, P. (1990). A repeating amino acid motif in *CDC23* defines a family of proteins and a new relationship among genes required for mitosis and RNA synthesis. *Cell* **60**, 307-317.

4. D'Andrea, L. D. & Regan, L. (2003). TPR proteins: the versatile helix. *Trends in Biochemical Sciences* **28**, 655-662.

Figure S1

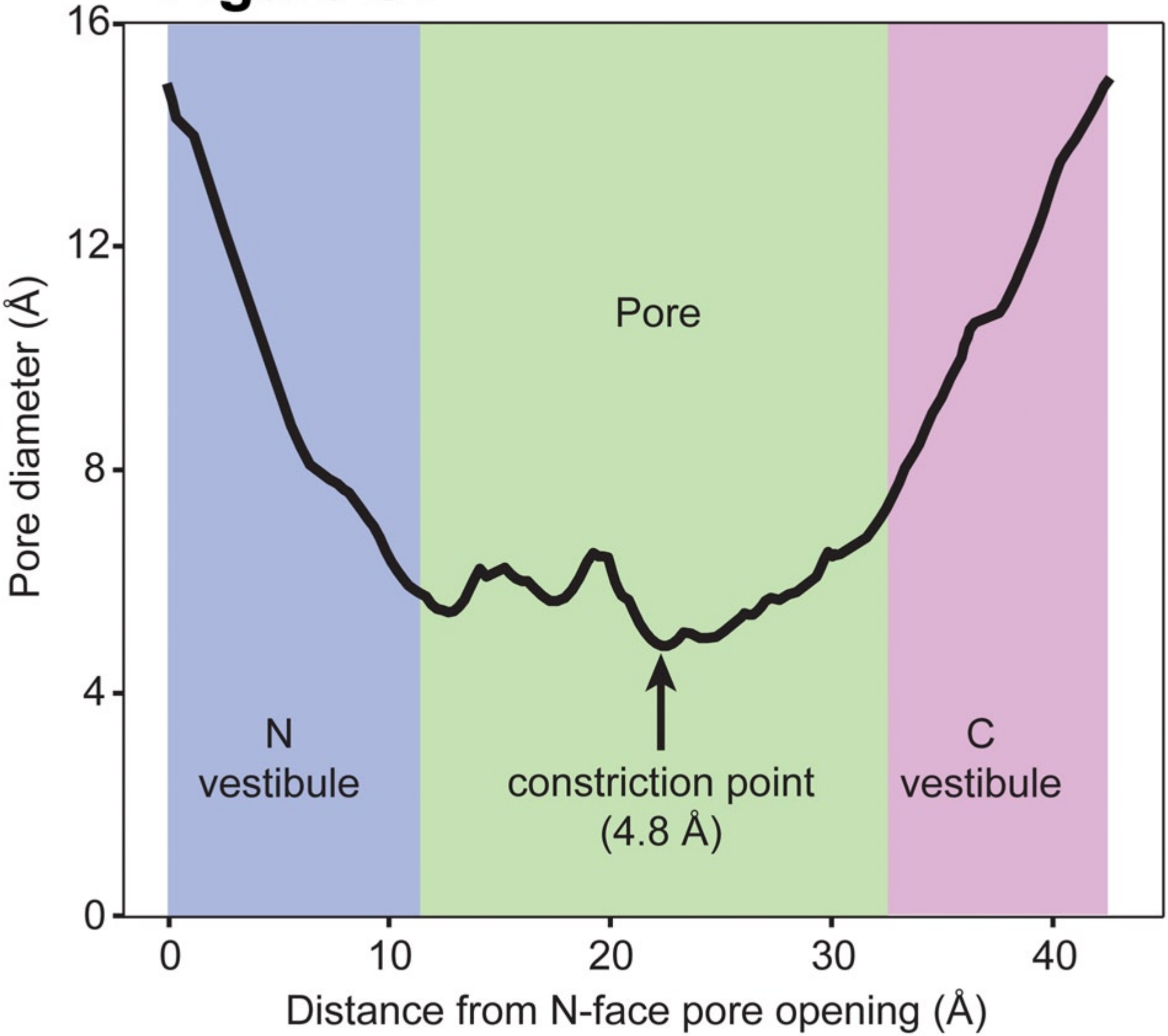
16
12
8
4
0
Pore diameter (Å)
Pore
N
vestibule
constriction point
(4.8 Å)
C
vestibule
0
10
20
30
40
Distance from N-face pore opening (Å)

Figure S2

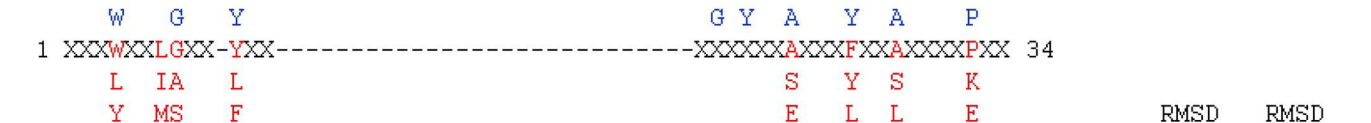
W G Y G Y A Y A P
1 XXXWXXLGXX-YXX----------XXXXXXAXXXFXXAXXXXPXX 34
L IA L S Y S K
Y MS F E L L E
RMSD RMSD
L 3GW4 2PL2
65 RGLSLAVGRL-YIMYANAFVQTPAQYLPEDEFEAQNEAYSRARKLYLRGARYALSSLETAYPG 126 65 1.2 1.2
151 VGILYWVGTG-YVAAFA----------LTPLGSALPDTVHAAVMMLERACDLWPSY 195 45 1.7 1.5
198 GAVWNVLTKF-YAAAPESF----------GGGMERAHTAFEHLTRYCSAH 236 39 0.6 0.7
238 PDHHITYADALCIPL----------NNRAGFDEALDRALAIDPES 272 35 0.9 0.6

Figure S3

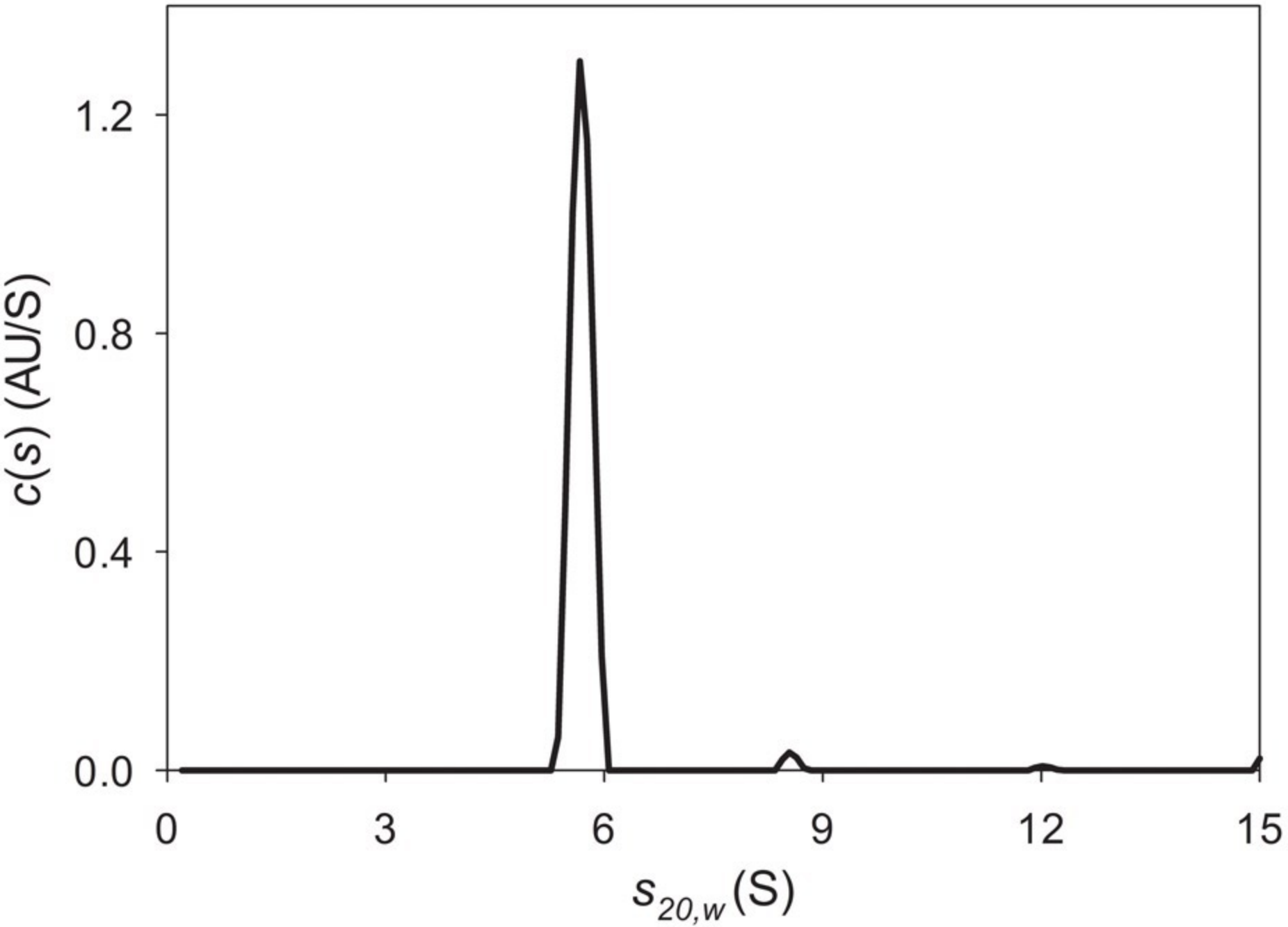

Figure S4

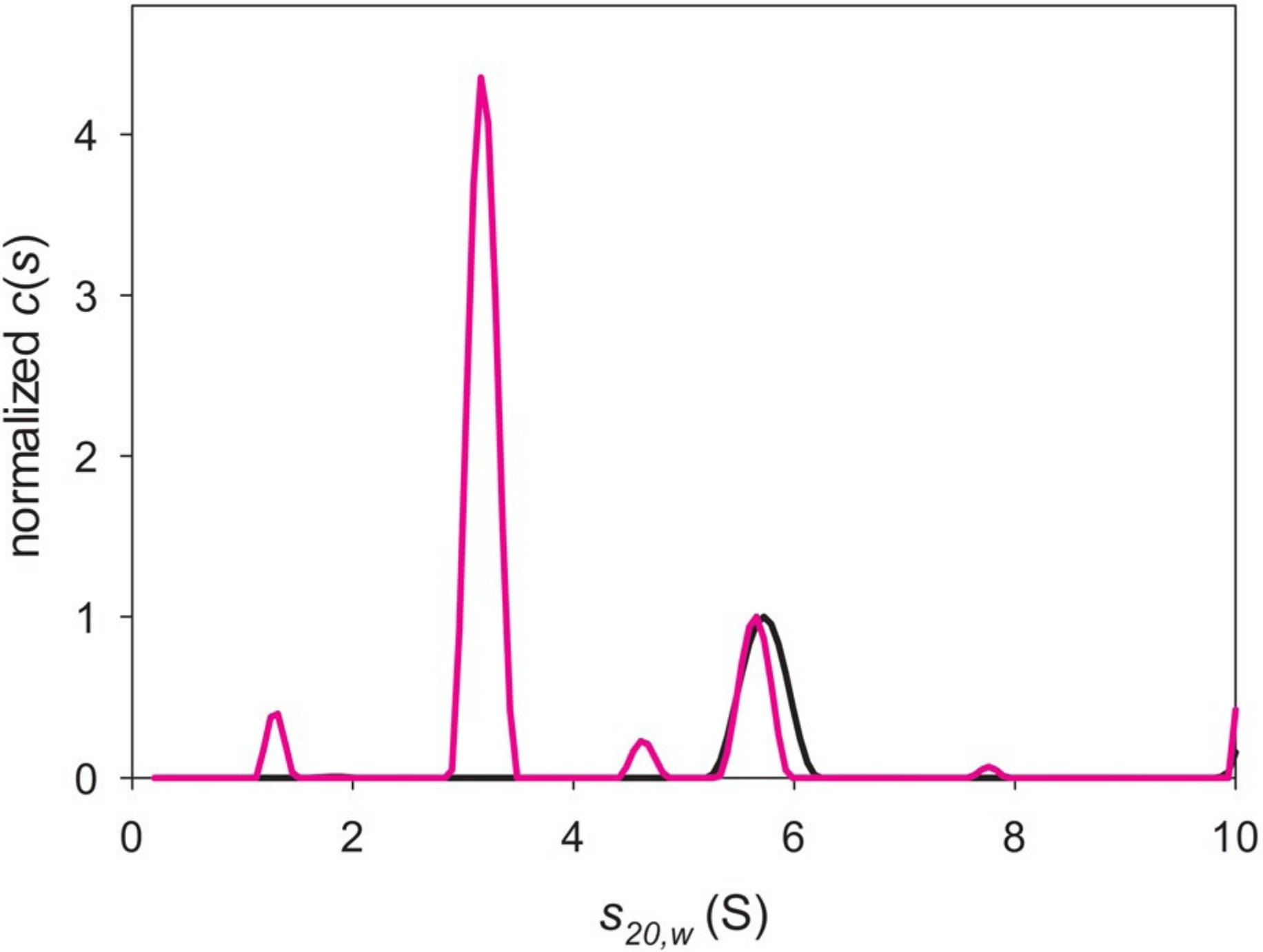

Figure S5

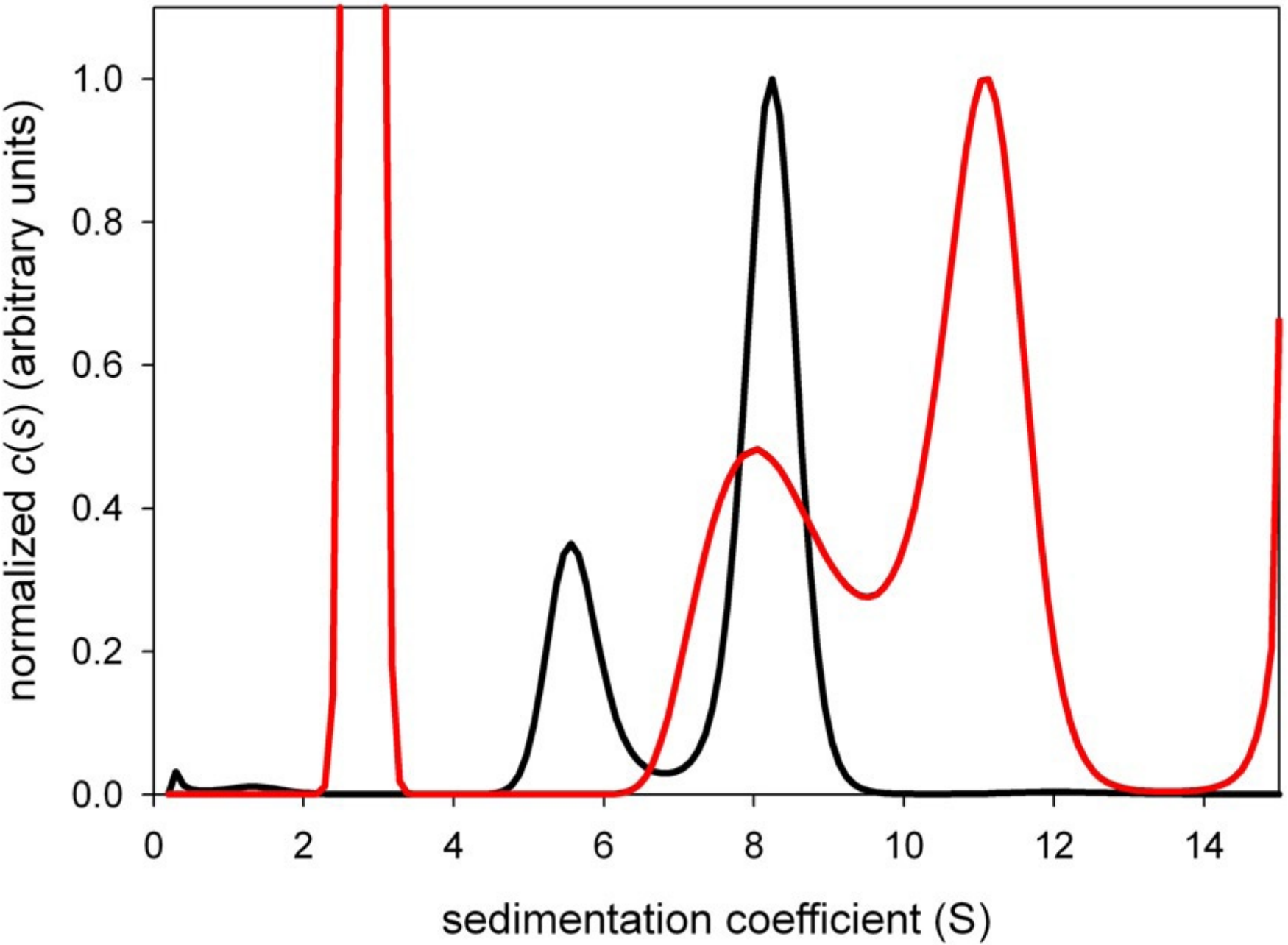
normalized c(s) (arbitrary units)
1.0
0.8
0.6
0.4
0.2
0.0
0
2
4
6
8
10
12
14
sedimentation coefficient (S)

Figure S6

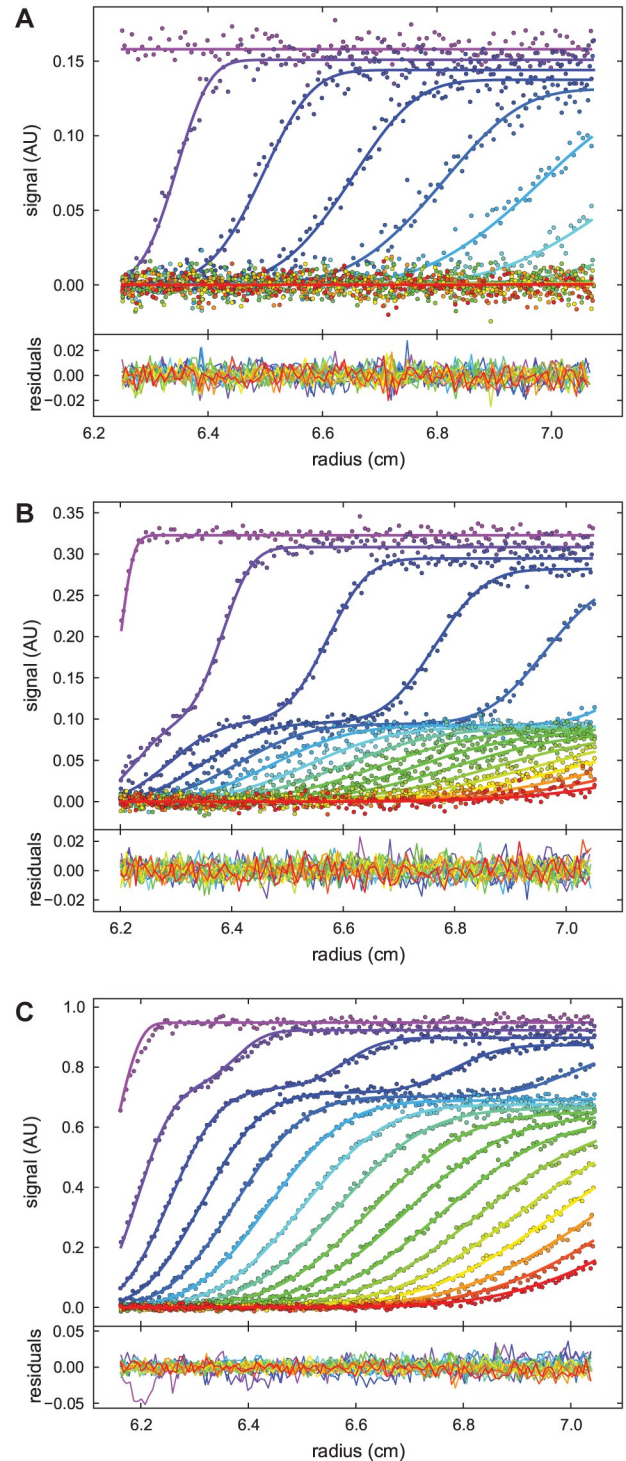
A
signal (AU)
0.15
0.10
0.05
0.00
residuals
0.02
0.00
−0.02
6.2
6.4
6.6
6.8
7.0
radius (cm)
B
signal (AU)
0.35
0.30
0.25
0.20
0.15
0.10
0.05
0.00
residuals
0.02
0.00
−0.02
6.2
6.4
6.6
6.8
7.0
radius (cm)
C
signal (AU)
1.0
0.8
0.6
0.4
0.2
0.0
residuals
0.05
0.00
−0.05
6.2
6.4
6.6
6.8
7.0
radius (cm)

Figure S7

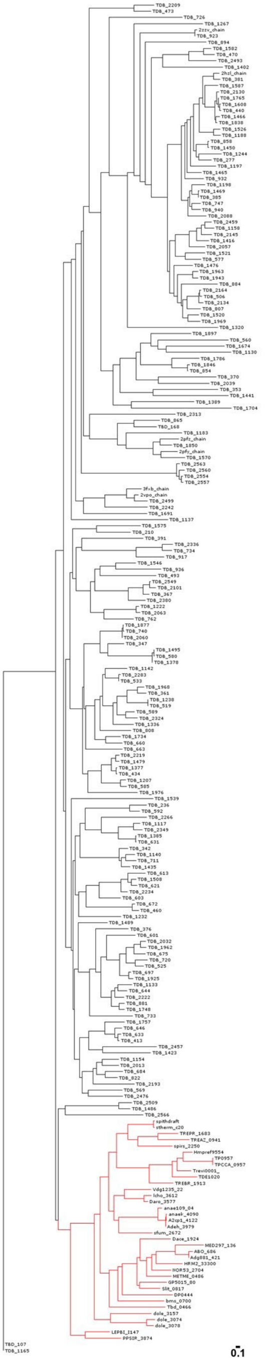
TDB_2209
TDB_473
TDB_726
TDB_1267
2zzv_chain
TDB_923
TDB_894
TDB_1582
TDB_470
TDB_2493
TDB_1402
2hzl_chain
TDB_381
TDB_1587
TDB_2130
TDB_1765
TDB_1608
TDB_440
TDB_1466
TDB_1838
TDB_1526
TDB_1188
TDB_858
TDB_1450
TDB_1244
TDB_277
TDB_1197
TDB_1465
TDB_932
TDB_1198
TDB_1469
TDB_385
TDB_747
TDB_940
TDB_2088
TDB_2459
TDB_1158
TDB_2145
TDB_1416
TDB_2057
TDB_1521
TDB_577
TDB_1476
TDB_1963
TDB_1943
TDB_884
TDB_2164
TDB_506
TDB_2134
TDB_807
TDB_1520
TDB_1969
TDB_1320
TDB_1897
TDB_560
TDB_1674
TDB_1130
TDB_1786
TDB_1846
TDB_854
TDB_370
TDB_2039
TDB_353
TDB_1441
TDB_1389
TDB_1704
TDB_2313
TDB_865
TBD_168
TDB_1183
2pfz_chain
TDB_1850
2pfy_chain
TDB_1570
TDB_2563
TDB_2560
TDB_2554
TDB_2557
3fxb_chain
2vpo_chain
TDB_2499
TDB_2242
TDB_1691
TDB_1137
TDB_1575
TDB_210
TDB_391
TDB_2336
TDB_734
TDB_917
TDB_1546
TDB_936
TDB_493
TDB_2549
TDB_2101
TDB_367
TDB_2380
TDB_1222
TDB_2063
TDB_762
TDB_1877
TDB_740
TDB_2060
TDB_347
TDB_1495
TDB_580
TDB_1378
TDB_1142
TDB_2283
TDB_533
TDB_1968
TDB_361
TDB_1238
TDB_519
TDB_589
TDB_2324
TDB_1336
TDB_808
TDB_1734
TDB_660
TDB_663
TDB_2219
TDB_1479
TDB_1377
TDB_434
TDB_1207
TDB_585
TDB_1976
TDB_1539
TDB_236
TDB_592
TDB_2266
TDB_1117
TDB_2349
TDB_1385
TDB_631
TDB_342
TDB_1140
TDB_711
TDB_1435
TDB_613
TDB_1508
TDB_621
TDB_2234
TDB_603
TDB_672
TDB_460
TDB_1232
TDB_1489
TDB_376
TDB_601
TDB_2032
TDB_1962
TDB_675
TDB_720
TDB_525
TDB_697
TDB_1925
TDB_1133
TDB_644
TDB_2222
TDB_881
TDB_1748
TDB_733
TDB_1757
TDB_646
TDB_633
TDB_413
TDB_2457
TDB_1423
TDB_1154
TDB_2013
TDB_684
TDB_822
TDB_2193
TDB_569
TDB_2476
TDB_2509
TDB_1486
TDB_2566
spithdraft
stherm_c20
TREPR_1683
TREAZ_0941
spirs_2250
Hmpref9554
TP0957
TPCCA_0957
Trevi0001_
TDE1020
TREBR_1913
Vdg1235_22
lcho_3612
Daro_3577
anae109_04
anaek_4090
A2cp1_4122
Adeh_3979
sfum_2672
Dace_1924
MED297_136
ABO_686
Adg881_421
HRM2_33300
NOR53_2704
METME_0486
GP5015_80
Slit_0817
DP0444
bms_0700
Tbd_0466
dole_3157
dole_3074
dole_3078
LEPBI_I147
PPSIR_3874
TBD_107
TDB_1165
0.1